

## Improving the Physical Model of GaAs Solar Cells

R.V. Zaitsev, M.V. Kirichenko

National Technical University «Kharkiv Polytechnic Institute», 2, Kyrpychov St., 61002 Kharkiv, Ukraine

(Received 28 June 2020; revised manuscript received 18 December 2020; published online 25 December 2020)

For large-scale GaAs-based solar cells using, it is necessary to increase their efficiency and reduce the cost of their manufacture. The existing model, which describes the processes in the semiconductor material, has significant simplifications and does not take into account a number of significant processes. The article considers the problem of processes in gallium arsenide based solar cells optimization, proposes to take into account the mechanisms of radiation, surface recombination, which have a significant impact and have not been previously considered in the physical model. The article also considers methods for taking into account the photon reabsorption, the effect of which in GaAs based solar cells is taken into account by building a model of photon reabsorption. The proposed model is based on the Steiner photon absorption model, which is successfully used for modeling single-junction GaAs solar cells, taking into account some boundary conditions considering recombination processes on the device inner surfaces. Calculations using the proposed model allowed us to offer an optimized solution of thin GaAs based solar cells with a good back surface mirror and reduced surface recombination.

**Keywords:** Photovoltaic converters, Solar cells, GaAs, Efficiency, Surface recombination, Photon recycle.

DOI: [10.21272/jnep.12\(6\).06015](https://doi.org/10.21272/jnep.12(6).06015)

PACS numbers: 84.60.Jt, 61.43.Bn

### 1. INTRODUCTION

Over the past 10 years, the development of single- and multi-junction GaAs based solar cells has been quite rapid, with the efficiency of such devices reaching 28.8 % and 39.5 % under AM 1.5 conditions, so they are the most efficient devices among solar cells. GaAs based solar panels are highly efficient devices, but they are too expensive for large-scale ground-based applications because of the device manufacturing high cost and the use of rare earth elements (In, Ga).

For widespread use of GaAs based solar cells, we need to increase their efficiency and reduce manufacturing costs. The existing model describing processes in a semiconductor material has significant simplifications and does not take into account a number of significant processes [1]. Therefore, to further improve such devices efficiency, there is a need to improve the physical model of such devices. For example, it is necessary to consider the recombination processes on all surfaces and photon re-absorption processes, which leads to a significant increase in the device efficiency. Improvement of a GaAs based solar cell physical model is a

very urgent task in the field of solar energy, including highly concentrated solar energy to create high effective hybrid photoenergy systems [2, 3].

### 2. GENERAL BASIS OF THE MODEL

#### 2.1 Photocurrent Density

The photocurrent density  $J_{ph}$  generated by photons at different wavelengths  $\lambda$  is the sum of three components. The first is the electron drift current in the  $p$ -type region  $J_n$ . The second is the hole drift current in the  $n$ -type region  $J_p$ . In the region of space charge, holes are accelerated to the  $p$ -type region, and electrons move to the  $n$ -type region, thus creating a photocurrent  $J_g$ . The photocurrent density can be described by the following relation:

$$J_{ph}(\lambda) = J_n(\lambda) + J_g(\lambda) + J_p(\lambda). \quad (2.1)$$

In the  $p$ -type region, the photocurrent density of nonequilibrium electrons at  $x = x_p$  for each wavelength  $\lambda$  is written as [4, 5]:

$$J_n(\lambda) = qD_n \left. \frac{d\Delta n}{dx} \right|_{x_p} = \frac{qF(\lambda)(1-R(\lambda))\alpha(\lambda)L_n \exp(-\alpha(\lambda)x_p)}{\alpha(\lambda)^2 L_n^2 - 1} \times \left[ \alpha(\lambda)L_n - \frac{\frac{S_n L_n}{D_n} \cosh h\left(\frac{x_p}{L_n}\right) + \sinh h\left(\frac{x_p}{L_n}\right) - \left(\frac{S_n L_n}{D_n} - \alpha(\lambda)L_n\right) \exp(-\alpha(\lambda)x_p)}{\frac{S_n L_n}{D_n} \sinh h\left(\frac{x_p}{L_n}\right) + \cosh h\left(\frac{x_p}{L_n}\right)} \right]. \quad (2.2)$$

In the  $n$ -type region, the photocurrent density of nonequilibrium holes at  $x = x_p + w$  is determined by the relation:

$$J_p(\lambda) = -qD_p \left. \frac{d\Delta p}{dx} \right|_{x_p+w} = \frac{qF(\lambda)(1-R(\lambda))\alpha(\lambda)L_p \exp(-\alpha(\lambda)(x_p+w))}{\alpha(\lambda)^2 L_p^2 - 1} \times \left[ \alpha(\lambda)L_p - \frac{\frac{S_p L_p}{D_p} \cosh\left(\frac{x_n}{L_p}\right) + \sinh\left(\frac{x_n}{L_p}\right) - \exp(-\alpha(\lambda)x_n) + \alpha(\lambda)L_p \exp(-\alpha(\lambda)x_n)}{\frac{S_p L_p}{D_p} \sinh\left(\frac{x_n}{L_p}\right) + \cosh\left(\frac{x_n}{L_p}\right)} \right]. \quad (2.3)$$

In the depletion region, the photocurrent density is the result of each photogenerated carrier from this layer collection and can be determined as follows:

$$J_g(\lambda) = -q \int_{x_p}^{x_p+w} G(x) dx = qF(\lambda)(1-R(\lambda)) \exp(-\alpha(\lambda)x_p) (1 - \exp(-\alpha(\lambda)w)) \quad (2.4)$$

where  $q$  is the electron charge,  $L_n$  and  $L_p$  are the electron and hole diffusion lengths, respectively,  $S_n$  and  $S_p$  are the electron and hole surface recombination rates, respectively,  $D_n$  and  $D_p$  are the electron and hole diffusion coefficients, respectively,  $R(\lambda)$  is the reflection coefficient,  $\alpha(\lambda)$  is the absorption coefficient, and  $F(\lambda)$  is the flux of incident photons.

The total solar cell photocurrent density is the result of integration across the entire solar spectrum:

$$J_{ph} = -q \int_{\lambda_{min}}^{\lambda_{max}} J_{ph}(\lambda) d\lambda. \quad (2.5)$$

The output current  $J(V)$  flowing through the solar cell when the bias voltage  $V$  is applied can be described using an exponential model as [6]:

$$J(V) = J_{ph} - J_s \left( \exp\left(\frac{V}{V_{th}}\right) - 1 \right), \quad (2.6)$$

where  $J_{ph}$  is the current density generated by the absorbed light and  $V_{th}$  is the thermal voltage determined by the ratio:

$$V_{th} = \frac{k_B T}{q}, \quad (2.7)$$

where  $k_B$  is the Boltzmann constant,  $T$  is the temperature of the solar cell.

The  $p$ - $n$  junction diode saturation current density ( $J_s$ ) is determined by the following relation:

$$J_s = q \left( \frac{p_{n0} D_p}{L_p} + \frac{n_{p0} D_n}{L_n} \right), \quad (2.8)$$

where  $n_{p0}$ ,  $p_{n0}$  are the concentrations of non-basic carriers (electrons and holes) at equilibrium in  $p$  and  $n$  regions, respectively.

The minority carrier diffusion coefficients in GaAs can be estimated as follows [7]:

$$D_n = 200 \frac{cm^2}{s},$$

$$D_p \approx \frac{V_T}{2.5 \cdot 10^{-3} + 4 \cdot 10^{-21} N_d}.$$

The minority carrier lifetime in the GaAs junction are determined by the following empirical formula:

$$\tau_n = 0.1 \mu s \text{ for } N_A \leq 10^{16} cm^{-3},$$

$$\tau_n = \frac{0.1}{\left[ \frac{(N_A - 10^{16})}{10^{16}} \right]^{0.5}} \mu s \text{ otherwise;}$$

$$\tau_p = 0.1 \mu s \text{ for } N_D \leq 10^{16} cm^{-3},$$

$$\tau_p = \frac{0.1}{\left[ \frac{(N_D - 10^{16})}{10^{16}} \right]^{0.5}} \mu s \text{ otherwise.}$$

## 2.2 Open-Circuit Voltage Ratio

The open-circuit voltage  $V_{oc}$  can be calculated from the equation as shown below [8]:

$$V_{oc} = \frac{k_B T}{q} \ln \left( \frac{J_{sc}}{J_s} \right), \quad (2.9)$$

where  $J_{sc}$  is the short-circuit current density equal to the photocurrent density at illumination.

The ratio for the diode saturation current  $J_s$ , according to [9], is:

$$J_s = 2 \cdot 10^{10} \left( \frac{D_p}{L_p N_D} + \frac{D_n}{L_n N_A} \right) T^3 \exp\left(\frac{-E_g}{k_B T}\right). \quad (2.10)$$

The bandgap  $E_g$  depends on intrinsic charge carrier ( $n_i$ ) concentration, which has the following form [10]:

$$n_i = 3.62 \cdot 10^{14} T^{\frac{3}{2}} \exp\left(\frac{-E_g}{2k_B T}\right). \quad (2.11)$$

## 2.3 Conversion Efficiency

The solar cell conversion efficiency is the ratio of the maximum output power  $P_m$  to the solar energy  $P_i$  going to its photoreceiving surface:

$$\eta = \frac{P_m}{P_i}. \quad (2.12)$$

The solar cell maximum output power  $P_m$  can be determined numerically from the maximum current  $J_m$  and maximum voltage  $V_m$ :

$$P_m = J_m V_m. \quad (2.13)$$

### 3. THE PROBLEM OF IMPROVING THE EFFICIENCY OF GaAs BASED DEVICES AND MODEL MISMATCHES

Photon absorption that is close to the optimum bandgap of the base semiconductor material is a fundamental element for high-efficiency solar cell realization. The proposed photon absorption model solves completely coupled nonlinear equations for quasi-one-dimensional electron and hole transport in crystalline semiconductor devices.

Shockley and Queisser introduced the optimal limit balance for solar cells in 1961 [11]. In general, the optimal balance model considers only two of its own losses, one is the unabsorbed energy loss because semiconductors cannot absorb photons whose energy is below the bandgap, and the other is the radiation recombination loss. In the real materials, there are other types of losses, such as thermal losses. The performance limit provided by this model is called the optimum balance. Shockley and Queisser calculated the optimal balance using the 6000 K black body spectrum and calculated own radiation flux using the optimal balance principle. Henry [12] has extended this approach using the standard AM 1.5 terrestrial spectrum. According to Henry's calculations [12], taking into account  $E_g$  and radiation recombination, the optimal  $E_g$  for one junction solar cells is 1.4 eV, as it is shown in Fig. 1.

The maximum efficiency of single-junction solar cells is 31 % at a solar radiation concentration  $C = 1$  and efficiency up to 37 %, 50 %, 56 % and 72 % for elements with 1, 2, 3 and 36 energy junctions (tandem elements), respectively, can be achieved at a radiation concentration  $C = 1000$  at room temperature (300 K). The GaAs bandgap is close to the optimum Shockley-Queisser value for single-junction solar cells with a maximum efficiency exceeding 30 %. Therefore, GaAs capable of reaching high efficiency ( $> 30\%$ ). Tandem solar cells on GaAs basis should also achieve the highest efficiency values [13, 14].

Today, it is possible to achieve sufficiently high-quality GaAs crystalline structures for solar cells in which the internal luminescence yield exceeds 99 % [15] and the dominant recombination mechanism is radiation recombination. Effectively reducing the effect of radiation recombination by increasing the re-absorption effect is one possible solution for maximum approach to Shockley-Queisser limit.

However, the modern mathematical apparatus, which is the basis of solar cell simulation programs, does not take into account a number of parameters. For example, the recombination parameters on the end surfaces, which are associated with single axis modeling and complex mechanisms of internal luminescence and reflection. In addition, the possibility of tandem structures with multiple junctions modeling has not taken into account. This does not allow us to model properties sufficiently accurately and in accordance with real modern devices and to find optimal design solutions. Moreover, the model itself needs refinement to take into account tandem structures and the necessary parameters and mechanisms.

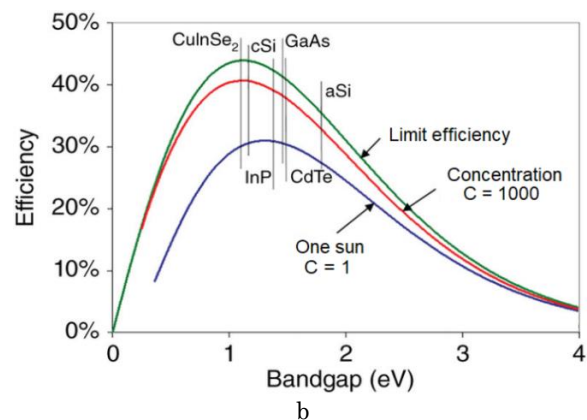
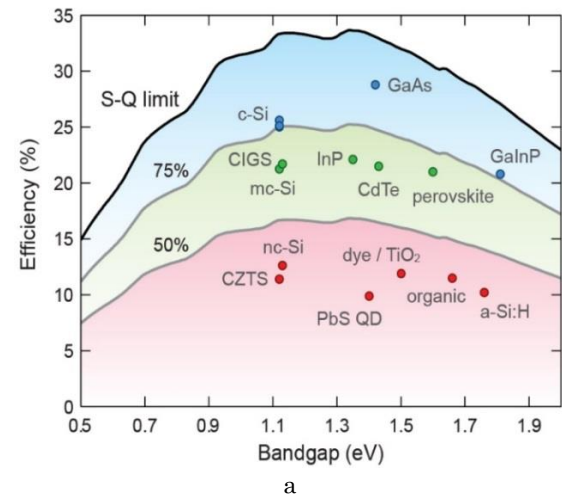


Fig. 1 – Dependence of solar cell efficiency on the basic semiconductor material bandgap at solar radiation concentrations  $C = 1$  (a) and  $C = 1000$  (b)

## 4. MATHEMATICAL MODEL MODERNIZATION

### 4.1 Recombination Consideration

Before modeling the recombination current effect on end surfaces (perimeter), it is necessary to understand the recombination mechanism on GaAs surface. The first model of such recombination was proposed [16, 17] for the  $p-n$  junction of the double AlGaAs heterostructure, where  $2k_B T$  recombination current amplitude does not correlate with area and this current is not mainly due to recombination occurring within the  $p-n$  junction, but instead recombination occurs along the crystal perimeter. According to research results, we obtained an analytical expression for perimeter recombination current on the  $p-n$  junction surface based on a number of assumptions, including Fermi level invariance, the density of donor and acceptor defects with uniform energy distribution over the bandgap, and the ratio of electron and hole densities on the surface that were assumed to be constant. The perimeter recombination current density decreases with distance from junction according to the simple diffusion equation with the average surface diffusion length  $L_s$ . The obtained  $L_s$  are of the same order of magnitude as the experimentally determined values, taking the conventional value  $S_0 = 4 \cdot 10^5$  cm/s.

Later authors of [18] considered recombination on

the  $p$ - $n$  junction surface similar to recombination in the depletion layer in the junction bulk using the Sah, Noyce, and Shockley (SNS) theory [19], and found a  $2kT$  recombination perimeter with an effective  $W_{eff}$  width. This width has the same expression as the bulk effective width  $W_{eff} = \pi kT/2eE$ , where  $E$  is the electric field normal to the transition and the recombination rate is maximum. The only difference is electric field amplitude. It was found that the electric field on the surface has the same direction but with a significantly reduced value. The authors suggested that the reason for this was the presence of charged states around the perimeter. The calculated  $W_{eff}$  value is about an order of magnitude smaller than the surface diffusion length  $L_s$  obtained in [16]. In [20], some adjustments were made to an earlier model [16], and it was concluded that  $2kT$  surface recombination current represents carrier drift diffusion from the junction depletion zone but not outside. This current was found to be dominant at small bias voltages, but at higher voltages, it became comparable to the recombination current resulting from injection from beyond the junction. The recombination current resulting from carrier injection within the quasi-neutral region has a  $kT$  behavior and may tend to  $2kT$  type at higher bias voltages. Carrier injection from the  $p$ - $n$  junction has two-dimensional nature. G.B. Lush [20], using a simplified analysis, reduced it to a one-dimensional problem. They obtained an analytical expression for the current around the perimeter outside the junction.

The most significant feature of surface states is that they typically introduce the energy level that lies in the semiconductor bandgap between the valence and conduction bands. These levels are usually evenly distributed throughout the bandgap. They arise either due to the crystal boundary action or due to the impurity's adsorption on the end surface. The surface recombination kinetics can be described by Shockley-Read-Hall statistics [21, 22] using the general expression for surface recombination rate:

$$R = N_{st} \frac{\sigma_n v_n \sigma_p v_p (n_s p_s - n_i p_i)}{\sigma_n v_n (n_s + n_i) + \sigma_p v_p (p_s + p_i)}, \quad (2.14)$$

where  $N_{st}$  is the surface state density at the  $\varepsilon_s$  level;  $\sigma_n$ ,  $\sigma_p$ ,  $v_n$  and  $v_p$  are the capture cross-section and thermal velocity of electrons and holes, respectively;  $n_i$  and  $p_i$  are the electron and hole densities that would exist if the corresponding Fermi level was at the surface level  $\varepsilon_s$ ;  $n_s$  and  $p_s$  are the electron and hole densities on the surface. Suppose that  $\varepsilon_s$  is close to bandgap middle, then  $n_i = p_i = n_i$  (defects with deep levels are recombination centers). We also assume that  $s_n = s_p = s$  and  $v_n = v_p = v$ , take the surface state density as  $N_s$  and assume that the states are isolated deep levels that have energies uniformly distributed over the bandgap. The surface is considered to be non-equilibrium so that  $n_s p_s \gg n_i^2$ . This allows to simplify the ratio for recombination:

$$R = S_0 \frac{n_s p_s}{n_s + p_s}, \quad (2.15)$$

where  $S_0 = \sigma v N_s$  represents the surface recombination rate.

## 4.2 Photon Recycling

Photon recycling describes the re-absorption and new electron-hole pair generation from photons arising at self-emission as a result of radiation recombination in semiconductors. These photons from self-emission can escape from the material or can be re-absorbed. For direct bandgap semiconductors, the absorption rate increases rapidly to  $1 \cdot 10^4 \text{ cm}^{-1}$ , as shown in Fig. 2, when the photon energy is higher than the semiconductor bandgap, as a result, the direct absorption effect is quite strong in direct bandgap semiconductors, according to the van Roosbroeck-Shockley ratio [22].

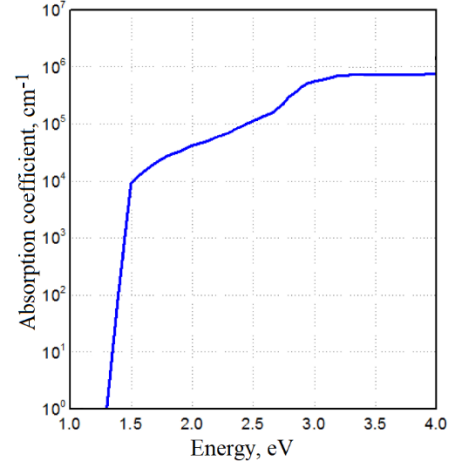


**Fig. 2** – GaAs absorption coefficient dependence on the photon energy

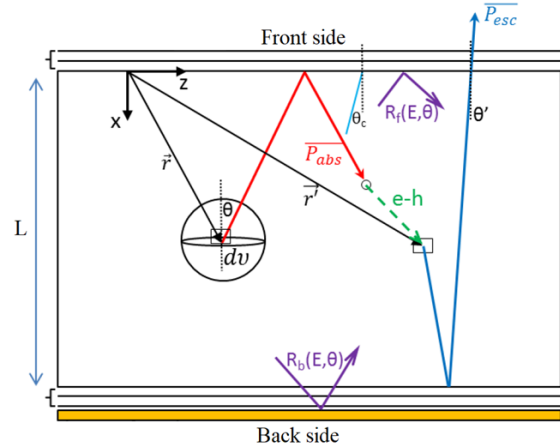


**Fig. 3** – Geometry of photon re-absorption modeling (red line – re-absorption after reflection from the frontal surface; green dotted line – electron-hole pair diffusion; blue line – photon output after double reflection; purple line – Fresnel reflection from the frontal and back surfaces)

$P_{esc}$  and  $P_{abs}$  represent the probability density of exit from the front surface and re-absorption, respectively, taking into account the initial emission in the elemental volume  $dv$ . The front reflection is

$$R_f = 1 - T_f = \begin{cases} 0: \vartheta < \vartheta_c \\ 1: \vartheta > \vartheta_c \end{cases},$$

where the critical angle  $\theta_c$  is defined as  $\sin \theta_c = 1/n$  and  $n$  is the GaAs refractive index.

The model calculates the probability of a photon escape from the front surface and its re-absorption into the GaAs solar cell. The spontaneous distribution of photon output is calculated as follows [23, 24]:

$$S(E) = \frac{2\alpha(E)n^2(E)E^2}{h^3c^2} \frac{1}{\exp\left(\frac{E-qV}{kT}\right)-1}, \quad (2.16)$$

where  $\alpha(E)$  is the layer absorption coefficient,  $n(E)$  is the layer refractive index,  $V$  is the bias voltage.

When  $E - qV \gg kT$ , it can be written:

$$S(E) \approx \frac{2\alpha(E)n^2(E)E^2}{h^3c^2} \exp\left(\frac{-E}{kT}\right) \exp\left(\frac{qV}{kT}\right). \quad (2.17)$$

Integrating by energy, the normalized photon output probability is as follows:

$$\hat{S}(E) = \frac{2\alpha(E)n^2(E)E^2 \exp\left(\frac{-E}{kT}\right) \exp\left(\frac{qV}{kT}\right)}{\int_0^\infty S(E)dE}. \quad (2.18)$$

The probability of a particular photon escape from the front surface is equal:

$$\overline{P_{esc}} = \int_0^\infty \hat{S}(E) \int_0^{\frac{\pi}{2}} \frac{T_f}{2\alpha L} \left( \frac{1 - e^{-\frac{L}{\cos\theta}}}{1 - R_f R_b e^{-\frac{2L}{\cos\theta}}} \right) \times \cos\theta \sin\theta d\theta dE \quad (2.19)$$

The probability of re-absorption is equal to

$$\overline{P_{abs}} = 1 - \int_0^\infty \hat{S}(E) \int_0^{\frac{\pi}{2}} \frac{\left(1 - e^{-\frac{\alpha L}{\cos\theta}}\right)}{\alpha L} \times \left(1 - \frac{1}{2} \left(1 - e^{-\frac{\alpha L}{\cos\theta}}\right) \frac{R_f + R_b + 2R_f R_b e^{-\frac{2\alpha L}{\cos\theta}}}{1 - R_f R_b e^{-\frac{2\alpha L}{\cos\theta}}}\right) \cos\theta \sin\theta d\theta dE, \quad (2.20)$$

the external luminescence efficiency  $\eta_{ext}$  is

$$\eta_{ext} = \frac{\eta_{int} \overline{P_{esc}}}{1 - \eta_{int} \overline{P_{abs}}}, \quad (2.21)$$

where  $\eta_{int}$  is the internal luminescence efficiency, which is calculated by the ratio:

$$\eta_{int} = \frac{R_{rad}}{R_{rad} + R_{nr}}, \quad (2.22)$$

where  $R_{rad}$  and  $R_{nr}$  are the radiation and non-radiation recombination rates, respectively.

With this model, the effective radiation factor can be calculated according to the ratio:

$$B = \left(1 - \eta_{int} \overline{P_{abs}}\right) \times B_0, \quad (2.23)$$

where  $B_0$  is the internal radiation coefficient and the value used here is  $5 \times 10^{-10} \text{ cm}^3/\text{s}$  [25].

## 5. CONCLUSIONS

This article considers and describes additional recombination mechanisms, such as surface recombination, radiation recombination, and non-radiative recombination, which were not previously considered in the physical model but have a significant impact. The photon recycling impact in GaAs based solar cells is taken into account by building a photon re-absorption model and such process modeling. Photon recycling plays an important role in approaching the balance point in semiconductor material, and its consideration will closer bring the model to full compliance. For multi-junction elements, the photon recycling model is constructed by modifying the Steiner model. This model has been successfully used to model single-junction GaAs solar cells with maximum efficiency by assuming some boundary conditions. In addition, a more detailed consideration of recombination processes on the device inner surfaces has been proposed, and in the case of low surface recombination, higher efficiency values can be achieved. For example, in thin GaAs based solar cells with a good rear-side mirror and reduced surface recombination, it is possible to obtain a higher open circuit-voltage without reducing the short-circuit current density increased by photon recycling.

## REFERENCES

1. M. Burgelman, K. Decock, S. Khelifi, A. Abass, *Thin Solid Films* **535**, 296 (2013).
2. R.V. Zaitsev, M.V. Kirichenko, G.S. Khrypunov, R.P. Migushchenko, L.V. Zaitseva, *2017 IEEE International Young Scientists Forum on Applied Physics and Engineering*, 112 (Ukraine: Lviv, 2017).
3. R.V. Zaitsev, M.V. Kirichenko, G.S. Khrypunov, D.S. Prokopenko, L.V. Zaitseva, *J. Nano-Electron. Phys.* **10** No 6, 06017 (2018).
4. S.M. Sze, K.Ng. Kwok, *Physics Semiconductor Devices* (John Wiley & Sons Inc.: 2007).
5. J.C. González, F.M. Matinaga, W.N. Rodrigues, M.V.B. Moreira, A.G. de Oliveira, *Appl. Phys. Lett.* **76**, 3400 (2000).
6. P. Singh, N.M. Ravindra, *Sol. Energy Mater. Sol. C.* **101**, 36 (2012).
7. J.J. Liou, W.W. Wong, *Sol. Energy Mater. Sol. C.* **28**, 9 (1992).
8. S. Chandra, A. Yadav, S. Agrawal, D.S. Chauhan, *Mater. Today: Proc.* **26**, 878 (2020).
9. A. Resfa, B.R. Menezla, M. Bougueneya, *Superlattice. Microst.* **72**, 352 (2014).
10. I.-W. Cho, S.H. Park, T.T. Nguyen, et al., *J. Alloy. Compd.* **832**, 154989 (2020).
11. W. Shockley, H.J. Queisser, *J. Appl. Phys.* **32**, 510 (1961).
12. R.Z. Falama, Hidayatullah, S.Y. Doka, *Optik* **187**, 39 (2019).
13. G.S. Khrypunov, G.I. Kopach, R.V. Zaitsev, A.I. Dobrozhan, M.M. Kharchenko, *J. Nano-Electron. Phys.* **9** No 2, 02008 (2017).
14. R.V. Zaitsev, V.R. Kopach, M.V. Kirichenko, E.O. Lukyanov, G.S. Khrypunov, V.N. Samofalov, *Functional Materials* **17** No 4, 554 (2010).
15. D. Ding, S.R. Johnson, J.-B. Wang, S.-Q. Yu, Y.-H. Zhang, *2008 Conference on Quantum Electronics and Laser Science*, 10172822 (2008).
16. K. Lia, Z. Liu, M. Tang, et al., *J. Crystal Growth* **511**, 56 (2019).

17. O. Larin, A. Kelin, R. Naryzhna et al., *Nucl. Radiation Safety* **79** No 3, 30 (2018).
18. M. Ochoa, C. Algora, P. Espinet-González, I. García, *Sol. Energy Mater. Sol. C.* **120(A)**, 48 (2014).
19. C.T. Sah, R.N. Noyce, W. Shockley, *Proc. IRE* **45** No 9, 1228 (1957).
20. G.B. Lush, *Sol. Energy Mater. Sol. C.* **93**, 1225 (2009).
21. A. Belghachi, *Microelectron. J.* **36**, 115 (2005).
22. W. van Roosbroeck, W. Shockley, *Phys. Rev.* **94**, 1558 (1954).
23. K.A. Minakova, A.F. Sirenko, V.V. Eremenko, et al., *Low Temp. Phys.* **42** No 5, 401 (2016).
24. M.V. Kirichenko, R.V. Zaitsev, A. Ivanov, D.S. Lobotenko, *International Young Scientists Forum on Applied Physics*, art. PECCS-5 (Ukraine: Dnipropetrovsk, 2015).
25. M. Brozel, *Gallium Arsenide, Springer Handbook of Electronic and Photonic Materials*, 499 (2007).

## Вдосконалення фізичної моделі сонячних елементів на основі GaAs

Р.В. Зайцев, М.В. Кіріченко

*Національний технічний університет «Харківський політехнічний інститут»,  
вул. Кирпичова 2, 61002 Харків, Україна*

Задля широкомасштабного використання сонячних елементів на основі GaAs необхідно підвищувати їх ефективність та знижувати витрати на їх виготовлення. Існуюча модель, що описує процеси у напівпровідниковому матеріалі, має значні спрощення та не враховує цілий ряд значних процесів. У роботі розглянута проблема оптимізації процесів у сонячних елементах на основі арсеніду галію, запропоновано врахування механізмів променевої, поверхневої рекомбінації, котрі мають суттєвий вплив і раніше в рамках фізичної моделі не розглядалися. Також у роботі розглянуто методи врахування повторного поглинання фотонів, вплив якого у сонячних елементах на основі GaAs враховується шляхом побудови моделі повторного поглинання фотонів. За основу запропонованої моделі обрано модель повторного поглинання фотонів Штейнера, яка успішно застосовується для моделювання одноперехідних сонячних батарей GaAs з урахуванням деяких граничних умов щодо врахування процесів рекомбінації на внутрішніх поверхнях приладу. Розрахунки з використанням запропонованої моделі дозволили запропонувати оптимізоване рішення тонких сонячних елементів на основі GaAs з хорошим дзеркалом на задній стороні та зниженою поверхневою рекомбінацією.

**Ключові слова:** Фотоелектричні перетворювачі, GaAs, ККД, Поверхнева рекомбінація, Повторне поглинання фотонів.